

人为气溶胶排放导致最近 80 年东亚夏季风在过去四个世纪以来空前减弱 *

刘禹^{1, 2, 3, 4}, 蔡文炬^{3, 5, 6, 1}, 孙长峰¹, 宋慧明^{1, 3}, Kim M. Cobb⁷, 李建平^{3, 5}, Steven W. Leavitt⁸, 吴立新³, 蔡秋芳^{1, 3}, 刘若时⁹, Benjamin Ng⁶, Paolo Cherubini¹⁰, Ulf Büntgen^{11, 10, 12}, 宋怡¹, 王国建^{3, 6}, 雷莺¹, 晏利斌¹, 李强^{1, 3}, 马永永¹³, 方丛羲¹, 孙军艳¹, 李旭祥⁹, Deliang Chen¹⁴, Hans W. Linderholm¹⁴

1. 中国科学院地球环境研究所 黄土与第四纪地质国家重点实验室, 西安 710061

2. 中国科学院第四纪科学与全球变化卓越创新中心, 西安 710061

3. 青岛海洋科学与技术试点国家实验室 - 海洋动力过程与气候功能实验室, 青岛 266237

4. 北京师范大学地球科学前沿交叉研究中心和全球变化研究联合中心, 北京 100875

5. 中国海洋大学物理海洋教育部重点实验室和青岛海洋科学与技术国家实验室, 青岛 266237

6. CSIRO Marine and Atmospheric Research, Aspendale, VIC 3195, Australia

7. School of Earth and Atmospheric Sciences, Georgia Institute of Technology, Atlanta, GA 30332, USA

8. The Laboratory of Tree-Ring Research, The University of Arizona, Tucson, AZ 85721, USA

9. 西安交通大学 人居环境与建筑工程学院, 西安 710049

10. Swiss Federal Institute for Forest, Snow and Landscape Research, CH-8903 Birmensdorf, Switzerland

11. Department of Geography, University of Cambridge, Cambridge CB2 3EN, UK

12. Global Change Research Centre and Masaryk University, 60177 Brno, Czech Republic

13. 陕西省气象局, 西安 710014

14. Climate Group, Department of Earth Sciences, University of Gothenburg, Box 100, SE-405 30 Gothenburg, Sweden

摘要: 亚洲夏季风 (Asian Summer Monsoon, ASM) 对亚洲数十亿人口的生存、亚洲生态系统和生物多样性的分布、以及农业生产 (粮食安全) 和工业活动影响严重。因此了解 ASM 过去时空变化及其动力学过程对陆地生态系统、水资源、森林和景观研究至关重要。近几十年, 器测记录显示以降水量为代表的 ASM 强度一直在减弱, 但这一减弱趋势的起始时间和动力学过程尚不清楚。为此, 第一次集成了 ASM 西部 - 中部边缘带 10 个对降水敏感的树木年轮宽度年表, 重建了公元 1566 年以来反映 ASM 强度变化的降水序列。

收稿日期: 2019-12-15; 录用日期: 2019-12-16; 网络出版: 2019-12-16

Received Date: 2019-12-15; Accepted Date: 2019-12-16; Online first: 2019-12-16

基金项目: 国家自然科学基金项目 (41630531); 大气重污染成因与治理攻关项目 (DQGG0104); 中科院项目 (QYZDJ-SSW-DQC021, XDPB05, GJHZ1777); 黄土与第四纪地质国家重点实验室项目 (SKLLQGZD1701)

Foundation Item: National Natural Science Foundation of China (41630531); National Research Program for Key Issues in Air Pollution Control (DQGG0104); Grant from Chinese Academy of Sciences (QYZDJ-SSW-DQC021, XDPB05, GJHZ1777), Grant from Institute of Earth Environment, Chinese Academy of Sciences, and State Key Laboratory of Loess and Quaternary Geology (SKLLQGZD1701)

通信作者: 刘禹, E-mail: liuyu@loess.llqg.ac.cn

Corresponding Author: LIU Yu, E-mail: liuyu@loess.llqg.ac.cn

引用格式: 刘禹, 蔡文炬, 孙长峰, 等. 2019. 人为气溶胶排放导致最近 80 年东亚夏季风在过去四个世纪以来空前减弱 [J]. 地球环境学报, 10(6): 527–542.

Citation: Liu Y, Cai W J, Sun C F, et al. 2019. Anthropogenic aerosols cause recent pronounced weakening of Asian Summer Monsoon relative to last four centuries [J]. Journal of Earth Environment, 10(6): 527–542.

*Copyright (2019) Wiley. Used with permission from (Liu et al, Anthropogenic Aerosols Cause Recent Pronounced Weakening of Asian Summer Monsoon Relative to Last Four Centuries, Geophysical Research Letters, John Wiley and Sons).

重建结果不仅捕捉到了 ASM 过去 4 个世纪以来强弱变化历史，也反映出历史上蝗灾与弱季风的关联。特别是发现了最近 80 年具有过去 448 年中前所未有的、最为强烈的、显著且持续时间最长的 ASM 强度减弱趋势。这一减弱趋势与在温室效应影响下 ASM 本该增强的预期大相庭径。耦合气候模型实验表明，北半球人为硫酸盐气溶胶排放的逐渐增加，对 ASM 减弱起了决定性作用。

关键词：东亚夏季风；树木年轮；降水重建；人为气溶胶；ASM 减弱趋势

Anthropogenic aerosols cause recent pronounced weakening of Asian Summer Monsoon relative to last four centuries

LIU Yu^{1, 2, 3, 4}, CAI Wenju^{3, 5, 6, 1}, SUN Changfeng¹, SONG Huiming^{1, 3}, Kim M. Cobb⁷, LI Jianping^{3, 5}, Steven W. Leavitt⁸, WU Lixin³, CAI Qiufang^{1, 3}, LIU Ruoshi⁹, Benjamin Ng⁶, Paolo Cherubini¹⁰, Ulf Büntgen^{11, 10, 12}, SONG Yi¹, WANG Guojian^{3, 6}, LEI Ying¹, YAN Libin¹, LI Qiang^{1, 3}, MA Yongyong¹³, FANG Congxi¹, SUN Junyan¹, LI Xuxiang⁹, Deliang Chen¹⁴, Hans W. Linderholm¹⁴

1. State Key Laboratory of Loess and Quaternary Geology, Institute of Earth Environment, Chinese Academy of Sciences, Xi'an 710061, China

2. CAS Center for Excellence in Quaternary Science and Global Change, Xi'an 710061, China

3. Laboratory for Ocean Dynamics and Climate, Pilot Qingdao National Laboratory for Marine Science and Technology, Qingdao 266237, China

4. Interdisciplinary Research Center of Earth Science Frontier and Joint Center for Global Change Studies, Beijing Normal University, Beijing 100875, China

5. Physical Oceanography Laboratory/CIMST, Ocean University of China and Qingdao National Laboratory for Marine Science and Technology, Qingdao 266237, China

6. CSIRO Marine and Atmospheric Research, Aspendale, VIC 3195, Australia

7. School of Earth and Atmospheric Sciences, Georgia Institute of Technology, Atlanta, GA 30332, USA

8. The Laboratory of Tree-Ring Research, The University of Arizona, Tucson, AZ 85721, USA

9. School of Human Settlements and Civil Engineering, Xi'an Jiaotong University, Xi'an 710049, China

10. Swiss Federal Institute for Forest, Snow and Landscape Research, CH-8903 Birmensdorf, Switzerland

11. Department of Geography, University of Cambridge, Cambridge CB2 3EN, UK

12. Global Change Research Centre and Masaryk University, 60177 Brno, Czech Republic

13. Shaanxi Meteorological Observatory, Xi'an 710014, China

14. Climate Group, Department of Earth Sciences, University of Gothenburg, Box 100, SE-405 30 Gothenburg, Sweden

Abstract: Background, aim, and scope The Asian Summer Monsoon (ASM) affects ecosystems, biodiversity, and food security of billions of people. In recent decades, ASM strength (as represented by precipitation) has been decreasing, but instrumental measurements span only a short period of time. The initiation and the dynamics of the recent trend are unclear. As a result, the properties of the recent ASM decreasing trend, including whether it is a part of a longer-term trend must be understood. Several forcing factors may affect the strength of the ASM, including solar variability, volcanic eruptions, and anthropogenic aerosols. So how aerosols and the ASM interact will also be examined given that concentration of aerosols in northwest China has been increasing over the past several decades. **Materials and methods** Here for the first time, we use an ensemble of 10 tree ring-width chronologies from the west-central margin of ASM, to reconstruct detail of monsoonal precipitation variability from July of previous year to June of current year (P_{JJ}) back to 1566 CE. The 10 tree ring-width chronologies are selected on the basis that they are sensitive only to rainfall, providing not only a higher-resolution but also an appropriate and direct proxy of the ASM over reconstruction from previous studies. **Results** The reconstructed P_{JJ} time series is a proxy for the ASM, measuring the ASM strength over its marginal zone. The reconstruction captures weak/strong ASM events, and it is found that historical severe droughts and locust plague disasters both appear during weak ASM events. Notably, we found an unprecedented 80-year trend of decreasing ASM strength within the context of the 448-year reconstruction, which is contrary to what is expected from greenhouse warming. Comparison of two sets of historical model experiments (10 runs each) with and without increasing anthropogenic aerosols shows that this unprecedented decreasing trend is likely due to increasing anthropogenic aerosols, highlighting that the ASM-weakening effect of increasing anthropogenic sulfate aerosols could more than offset

the ASM-enhancing effect of increasing greenhouse gases. **Discussion** Modeling is the only way to identify likely causes of the decreasing trend, and the results support a mechanism that would otherwise be difficult to measure directly. Our work further confirmed that anthropogenic aerosol's role in the ASM weakening in a longer period of 1934—2013, compared with previous study which spans 44 years (1958—2001). Besides the increase of sulfate aerosols, other factors, such as PDO and NAO, might have influences on the monsoon weakening, especially during historical periods without anthropogenic aerosols. **Conclusions** Our reconstruction provides an important time series to study the ASM over the past 448 years. The time series confirms known properties of the ASM (e.g., the 24-year frequency spectrum), reproduces known historical extreme climate events, and offers opportunities to understand less-known events. Further, the reconstruction can contribute to the debate regarding the recent behavior of the ASM and help evaluate the relative importance of anthropogenic radioactive forcing factors. **Recommendations and perspectives** We expect that the time series will find a wide range of utility for understanding past climate variability and for predicting future climate change.

Key words: the Asian Summer Monsoon; tree ring; reconstruction; anthropogenic aerosols; ASM decreasing trend

亚洲夏季风(ASM)是由季节性太阳辐射驱动引起的海陆热力差异而形成。季风降水与中国大部分地区,尤其是季风活动边缘带的工农业生产密切相关。季风活动边缘带与中国200 mm至400 mm降水等值线基本平行(图1a; Liu et al, 2014),它也是介于干旱与半干旱、沙漠与黄土带之间的过渡带。受ASM强烈影响,夏季降水占区域年降水的70%—90%(Wang, 2006)。掌握ASM时空变化及相关动力学过程,对理解陆地生态系统、水资源、森林及景观都显得至关重要(Wang, 2006; Piao et al, 2010; Liu et al, 2017)。太阳活动、火山爆发和人为气溶胶等若干强迫因素都可能影响ASM的强度,其中尤其值得关注的是人为气溶胶这一强迫因素。在过去几十年中,中国,特别是中国西北部的气溶胶浓度一直在增加(Lau and Kim, 2006; Bollasina et al, 2011; Zhu et al, 2012a; Ganguly et al, 2012; Song et al, 2014; Kim et al, 2016; Cai et al, 2017)。然而,气溶胶和ASM如何相互作用,这一互动机制尚未完全厘清(Li et al, 2016; Wu et al, 2016)。

了解ASM变化历史对于探索其归因和预测未来的变化都非常重要。基于现代观测记录,对ASM系统的子系统成分、起始时间、季节周期、水汽来源、动力学过程等方面进行了大量研究(Waliser et al, 2003; Ding and Chan, 2005; Li et al, 2015; Ueda et al, 2015)。目前的结论是自上世纪70年代末以来,ASM呈减弱趋势(Wang, 2001)。但是要进一步研究其长时间的动态变化过程,确定这种变化是由自然还是人为因素造成,那

么将这一减弱趋势置于长期历史背景下来研究则至关重要。目前的减弱是否是长期减弱趋势的一部分?然而观测记录覆盖时段过短,无法探寻气候变化长期趋势。

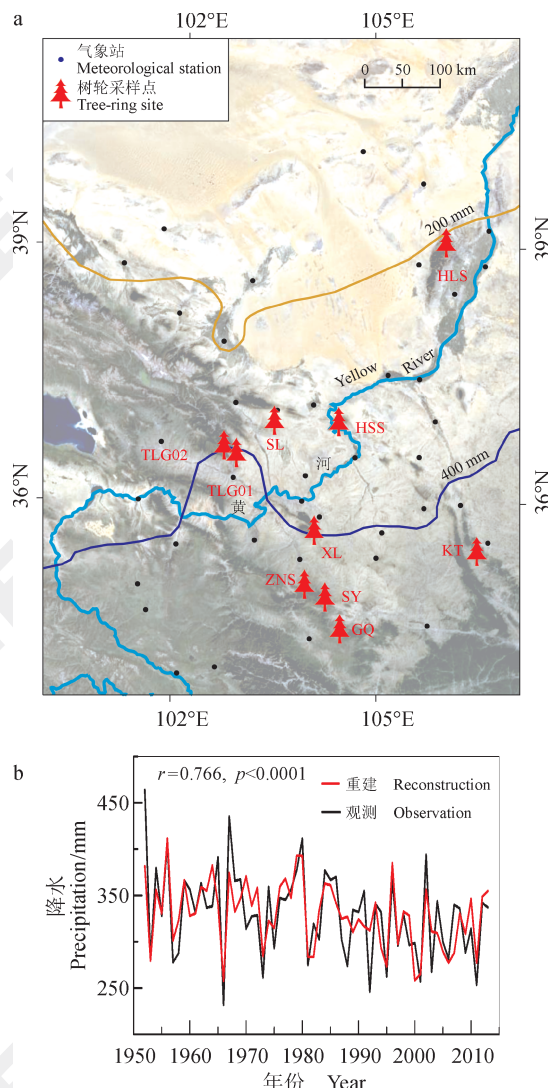
在本文研究中,基于中国黄土高原西部的10个对降水非常敏感的树木年轮宽度年表,重建了自公元1566年以来长达448年的ASM降水序列;讨论过去前所未有的近80年ASM显著减弱趋势,探讨这一趋势与持续增加的人类气溶胶之间的关系。

1 材料和方法

1.1 树轮年表和气象数据

研究中采用ASM边缘地区的10个树轮年表,共310棵树(含584根样芯,图1a和表1)。这些年表中,管涔山年表尚未发表;寿鹿山、首阳山、竺尼山和吐鲁沟的年表均已发表(Liu et al, 2013a; Liu et al, 2013b; 宋慧明等, 2017; Sun et al, 2018);贺兰山、崆峒山、兴隆山、哈思山的年表为新近更新数据,更新前的数据已发表(Liu et al, 2005; Song and Liu, 2011; Liu et al, 2013c; Ma et al, 2015)。每个样点至少采集20棵树,年轮宽度使用精度为0.001 mm宽度测量仪进行测量。根据树木在相同时期和相同气候条件下表现出相似的年际生长变化这一基本原理(Fritts, 1976),运用交叉定年方法确定每一轮的日历年。所得每一点的年表都能较好地反映当地降水信号(Liu et al, 2005; Fang et al, 2010; Song and Liu, 2011; Liu et al, 2013a; Liu et al, 2013b; Liu et al, 2013c; Ma et al, 2015;

宋慧明等, 2017; Sun et al., 2018), 且各年表之间具有显著相关性(表 2)。



a: 10 个树轮样点 (红色树形标识) 和 ASM 北部活动边缘带的 39 个气象站点 (黑色圆点, 均显示在图中); 黄线为 200 mm 降水等值线, 蓝线为 400 mm 降水等值线。b: 1952—2013 年树轮重建 P_{JJ} 序列 (红线) 与 P_{JJ} 观测序列 (黑线) 的对比。

a: location of 10 tree ring sampling sites (red tree shapes) and 39 meteorological stations (all within the box plotted) at the northern margin of the ASM (black dots). The yellow line is the precipitation isohyet of 200 mm, and the blue is 400 mm. b: comparison of reconstructed (red line) by tree rings and the observed (black line) precipitation data of P_{JJ} during 1952—2013.

图 1 亚洲夏季风 (ASM) 降水 P_{JJ} (上年七月至当年六月降水总量) 观测站点与树轮采样点分布

Fig.1 Location of the Asian Summer Monsoon (ASM) rainfall observations P_{JJ} (Precipitation from July of previous year to June of current year) and tree ring samples

在研究中, 将 10 个样点的所有样芯合并使用

ARSTAN 程序 (Cook and Kairiukstis, 1990) 生成能够代表 ASM 边缘带的树轮年表。选用直线或负指数函数拟合树木生长趋势, 将每个样芯每一轮的原始测量值除以生长趋势进行标准化, 采用双权重平均法合成区域年表。ARSTAN 程序能够生成三种类型的区域年表: 标准年表 (STD)、差值年表 (RES) 和自回归年表 (ARS)。因为 STD 同时包含高频和低频信息, 最终选择 STD 进行进一步分析和研究。按照年表子样本强度 >0.85 (Wigley et al., 1984) 确定的年表有效时段为 1566—2013 年 (起始年代包含 9 根样芯), 并以该时段作为年表的重建时段 (图 2 和表 3)。

气象数据采用 ASM 西北缘 39 个气象站 1951—2013 年的降水和气温观测数据 (图 1a)。为了研究 ASM 边缘带树木生长对区域气候的响应情况, 采用全部气象站的均值来代表区域气候条件。研究区逐月降水量和气温如图 3a 所示。

1.2 转换方程的建立及检验

相关函数分析表明, 在 1952—2013 年所有气象站共同观测期间, 区域树轮年表对季风边缘带的降水响应明显, STD 与上年 7 月至当年 6 月的区域降水呈显著正相关 (P_{JJ} , 图 3b)。因此运用线性回归模型设计转换方程:

$$P_{JJ} = 140.644 \times W_t + 198.455$$

($r = 0.766$, $R^2 = 0.586$, $R_{adj}^2 = 0.579$, $N = 62$, $p < 0.0001$)

式中: W_t 代表 t 年的 STD 值。

在校验期 (1952—2013 年), 重建降水对观测降水的方差解释量为 58.6%。图 1b 表明重建降水与观测记录相关较好。利用分段检验法对重建方程的稳定性和可靠性进行检验 (Cook et al., 1999; Fritts, 1991)。分别采用 1952—1981 年和 1984—2013 年的气候数据进行建模, 并用剩余的 1982—2013 年和 1952—1983 年的数据对相应的建模结果进行检验。检验过程用到的参数有相关系数 (r)、方差解释量 (R^2)、符号检验 (ST)、误差缩减值 (RE)、效率系数 (CE)、乘积均值检验 (t) 等。检验统计参数表明回归模型具有较高的稳定性和可靠性 (表 4; Cook et al., 1999), 特别是 RE 和 CE 值均远大于 0。区域年表与重建 P_{JJ} 序列之间线性相关, 表明 P_{JJ} 重建序列能够反映 ASM 边缘带的区域降水情况。

表 1 亚洲夏季风北部活动边缘带 10 个树轮采样点信息

Tab.1 Information about the 10 tree-ring sites from the northern margin of the Asian Summer Monsoon

序号 No.	样点 Site	树种 Species	纬度 Latitude	经度 Longitude	海拔 Elevation /m	起始年 Starting year	结束年 Ending year	年代长度 Years	树芯数量 Cores	文献 References
1	贺兰山 Mt. Helan (HL)	松 Pine	38.31°N	105.46°E	2400—2500	1742	2013	272	125	Liu et al (2005) **
2	寿鹿 Shoulu (SL)	云杉 1 Spruce 1	37.08°N	103.44°E	2498	1828	2007	180	55	Liu et al (2013a) *
3	吐露沟 Tulugou (TLG01)	松 Pine	36.63°N	102.79°E	2370	1721	2008	288	56	Liu et al (2013b) *
4	吐露沟 Tulugou (TLG02)	松 Pine	36.69°N	102.73°E	2146	1726	2008	283	51	Liu et al (2013b) *
5	兴隆山 Mt. Xinglong (XL)	云杉 1 Spruce 1	35.78°N	104.07°E	2314	1580	2013	434	48	Liu et al (2013c) **
6	崆峒山 Mt. Kongtong (KT)	松 Pine	35.50°N	106.50°E	1500—2123	1547	2013	467	73	Song and Liu (2011) **
7	哈思山 Mt. Hasi (HS)	松 Pine	37.00°N	104.40°E	2400—2700	1666	2013	348	62	Ma et al (2015) **
8	贵清山 Mt. Guiqing (GQ)	松 Pine	34.63°N	104.47°E	2460	1492	2011	520	56	***
9	首阳山 Mt. Shouyang (SY)	云杉 2 Spruce 2	34.99°N	104.24°E	2340	1683	2013	331	29	Sun et al (2018) *
10	竺尼寺 Zhunisi (ZNS)	松 Pine	35.14°N	103.94°E	2420	1880	2013	134	29	宋慧明等 (2017) (Song et al (2017))

松: 油松 (*Pinus tabulaeformis* Carr.) ; 云杉 1: 青海云杉 (*Picea crassifolia* Kom.) ; 云杉 2: 紫果云杉 (*Picea purpurea* Mast.) 。

* 年表数据已发表; ** 新近更新年表数据, 原先该地年表数据已发表; *** 年表数据未发表。

Pine: *Pinus tabulaeformis* Carr.; Spruce 1: *Picea crassifolia* Kom.; Spruce 2: *Picea purpurea* Mast.

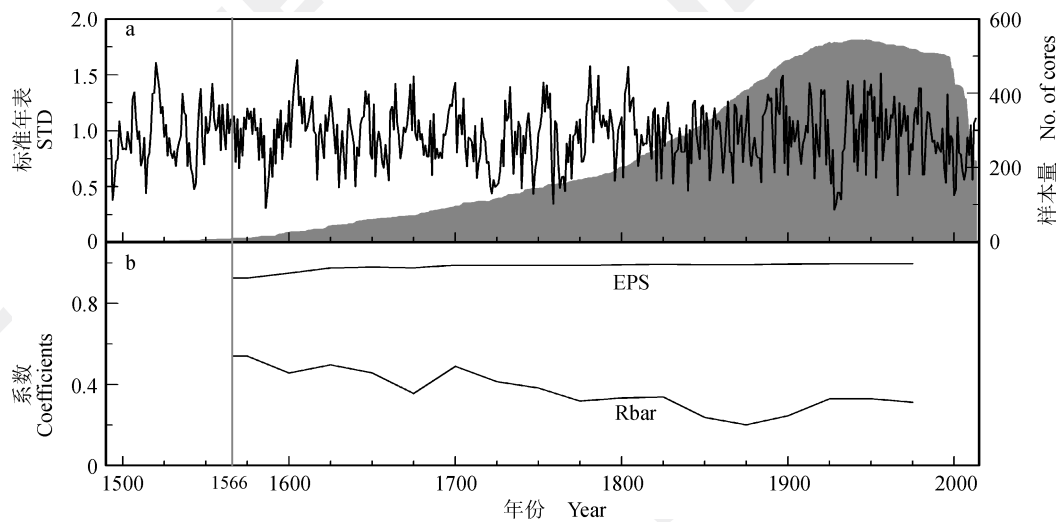
* represents that the chronology was published data; ** represents that the chronology was update data and the old chronologies from these sites were published; *** represents that the chronology was unpublished data.

表 2 所有年表间两两相关情况
Tab.2 Correlations among all chronologies

	贵清山 Mt. Guiqing	崆峒山 Mt. Kongtong	兴隆山 Mt. Xinglong	哈思山 Mt. Hasi	首阳山 Mt. Shouyang	吐露沟 01 Tulugou 01	吐露沟 02 Tulugou 02	贺兰山 Mt. Helan	寿鹿山 Mt. Shoulu
崆峒山 Mt. Kongtong	0.51, 465								
兴隆山 Mt. Xinglong	0.50, 432	0.37, 434							
哈思山 Mt. Hasi	0.41, 346	0.35, 348	0.45, 348						
首阳山 Mt. Shouyang	0.45, 329	0.34, 331	0.47, 331	0.25, 331					
吐露沟 01 Tulugou 01	0.40, 288	0.37, 288	0.46, 288	0.53, 288	0.29, 288				
吐露沟 02 Tulugou 02	0.27, 283	0.24, 283	0.45, 283	0.44, 283	0.26, 283	0.63, 283			
贺兰山 Mt. Helan	0.23, 270	0.25, 272	0.28, 272	0.45, 272	0.25, 272	0.42, 267	0.37, 267		
寿鹿山 Mt. Shoulu	0.32, 180	0.36, 180	0.51, 180	0.58, 180	0.29, 180	0.62, 180	0.53, 180	0.41, 180	
竺尼寺 Zhunisi	0.49, 131	0.61, 133	0.57, 133	0.31, 133	0.48, 133	0.43, 128	0.44, 128	0.27, 133	0.35, 127

表中含相关系数 r 与样本量 n , 所有 p 值小于 0.001。

r, n , and all at $p < 0.001$.



a: 年表与样本量; b: 滑动表达样本信号 (EPS) 与序列间公共时段的树间平均相关 (Rbar)。

a: chronology and sample size; b: running expressed population signal (EPS) and average correlation among trees for the common overlap period among series (Rbar).

图 2 亚洲夏季风边缘区域树轮宽度标准年表

Fig.2 Regional tree-ring standard chronology in the fringe region of the Asian Summer Monsoon

表 3 亚洲夏季风北部边缘区域树轮宽度标准年表 (STD) 的统计特征

Tab.3 Statistical characteristics of the regional tree-ring width standard chronology (STD) in Asian Summer Monsoon northern margin

统计量	Statistics	STD
均值	Mean sensitivity	0.26
标准差	Standard deviation	0.26
偏度	Skewness	-0.08
峰度	Kurtosis	2.60
一阶自相关系数	First-order autocorrelation	0.36
所有序列间平均相关系数	Mean correlation among all series	0.36
表达样本信号	Expressed population signal (EPS)>0.85	1566 年 (9 个芯)
		1566 (9 cores)

2 结果

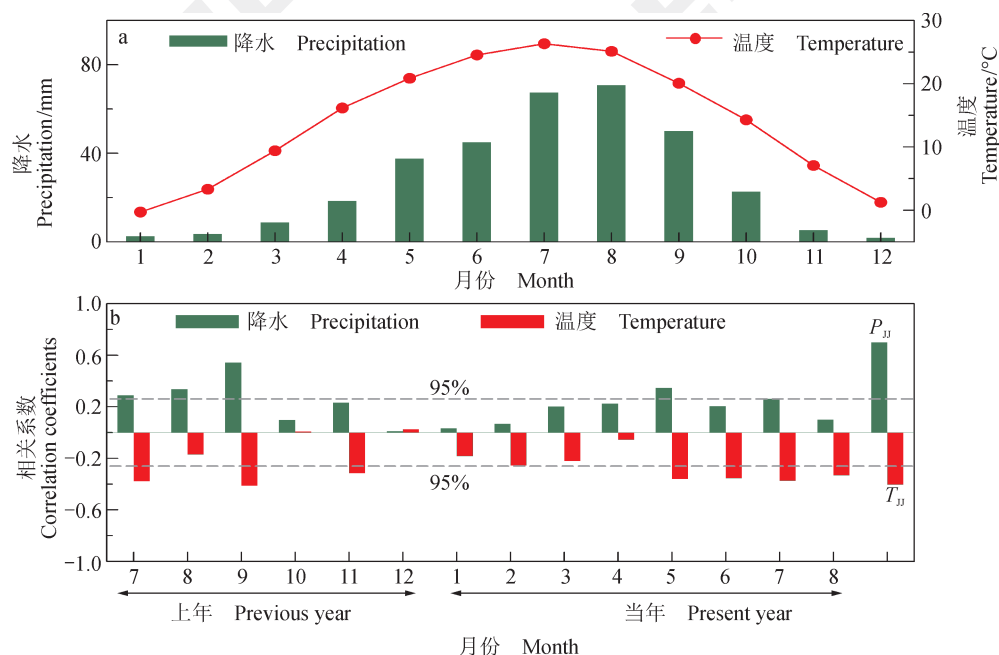
2.1 东亚夏季风水汽来源和重建应用

ASM 北缘地区降水来源于南亚季风和东亚季风的水汽输送 (Ding and Chan, 2005)。与长江下游相似, ASM 其他区域 7—9 月 700 hPa 以下 (海拔 3000 m 及以下) 的水汽来源于印度洋和西太平洋。然而, 由于对横贯东亚的太平洋 - 日本模式的罗斯比波响应, 在弱 ASM 期间, 北太平洋上空存在反气旋异常, 同时在其北部存在一个气旋异常 (Feng et al., 2014)。气旋异常的西侧存在北风异常。这种环流异常虽使得中国北方水汽输送减少, 但会增加长江下游水汽辐合 (Wang et al., 2008)。但是, 由于辐合异常呈带状分布, 在不同的大气环流异常下, 辐合异常可能并不位于同一纬度 (Wang

et al., 2001; Feng et al., 2014)。一旦 ASM 减弱, 由于水汽补充不足, 北方可能会经历干旱, 但南方却不一定各地都呈湿润状态。因此, 北部边缘地区的降水对 ASM 的增强 / 减弱更为敏感 (Ding et al., 2008; Wang et al., 2008); 从 1951—2013 年季风边缘地区 39 个站点的观测结果来看, 上年 7—9 月的降水量占上年 7 月到当年 6 月降水总量 (P_{JJ}) 的 56.7%。因此, 北部边缘地区的降水可指示 ASM 强度变化。此外, 观测 P_{JJ} 与中国北方大部分地区 7—9 月降水存在显著的相关性 (图 4a)。在同一时段, 重建 P_{JJ} 与上一年 7 月、8 月和 9 月的实测降水相关性最强, 这也是 ASM 活动强烈的季节 (图 5)。重建 P_{JJ} 序列与前一年 7—9 月降水的相关性达到 0.574。同时, 重建 P_{JJ} 序列与北方前

一年7—9月降水也显著相关(图4b)。因此,重建的 P_{JJ} 序列可视为指示ASM强度变化的一个代用指标,指示ASM在其活动边缘区域上的强度(图4),高 P_{JJ} 值意味着较强的ASM活动(Ding et al., 2008)。由于重建 P_{JJ} 是代表ASM边缘地区的,而其他ASM指数主要是针对在东亚/中国或南亚/中国的,因此它们之间会存在一定差异(Li and Zeng, 2002; Wang and Fan, 1999)。目前,基于树轮的ASM重建研究大多是仅基于一两条青

藏高原地区的树轮序列(Li et al., 2008; Griebinger et al., 2011; Xu et al., 2012)所得的结果。尽管该区域有一条季风序列使用了季风区多个样点的树轮资料,但却是主要针对南亚季风变化(Shi et al., 2014; Shi et al., 2017)的研究。本文则使用了10个树轮年表进行重建研究,且所选年表对ASM边缘带的季风降水均存在较强响应,因此本文的重建序列对季风变化更为敏感,也与其他ASM重建序列有明显差异(图6)。



a: 39个气象站平均降水与平均气温记录的月分布(1951—2013年)。b: 轮宽指数与亚洲夏季风北部边缘区39个气象站月均气温(红柱)和降水(绿柱)记录的相关分析(1951—2013年)。 P_{JJ} 为上年七月至当年6月的年降水量。虚线为95%置信限。

a: Monthly precipitation and temperature distribution of the averaged observation data from 39 meteorological stations (1951—2013). b: Correlation between ring width index and monthly averaged mean temperature (red bars) and precipitation (green bars) meteorological data from 39 stations at the northern margin of the Asian Summer Monsoon (1951—2013). P_{JJ} is the precipitation from previous July to current June. The dashed line is the 95% confidence limit.

图3 气象数据与相关函数分析
Fig.3 Climatic data and correlation analysis

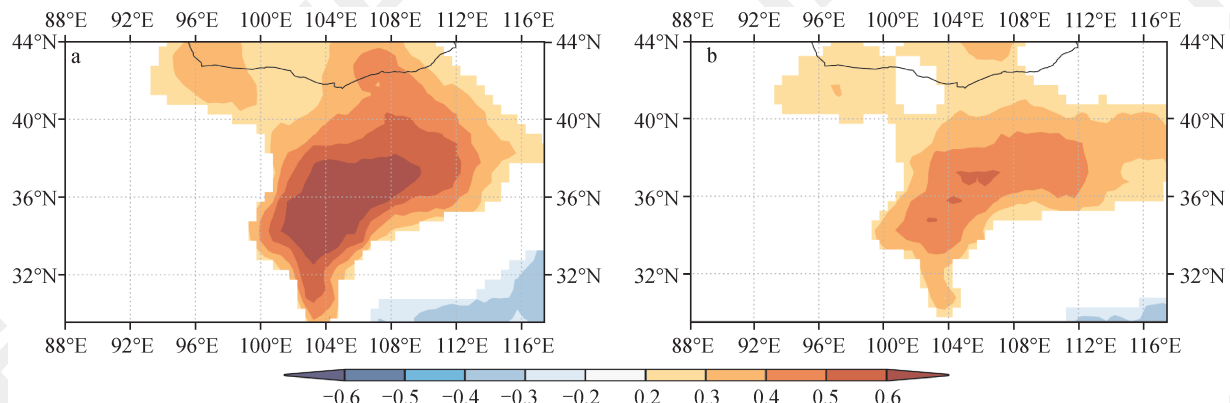
表4 P_{JJ} 重建的分段检验统计结果

Tab.4 Statistics of the split calibration-verification model for the P_{JJ} reconstruction

建模期 Calibration					校验期 Verification								
时段	Period	r	R^2	ST	t	时段	Period	r	R^2	RE	CE	ST	t
1952—1981	1952—1981	0.802**	0.643	22*	4.59	1982—2013	1982—2013	0.661**	0.437	0.57	0.36	21	6.16
1984—2013	1984—2013	0.686**	0.471	21*	6.22	1952—1983	1952—1983	0.787**	0.619	0.66	0.59	24**	4.73
1952—2013	1952—2013	0.766**	0.586	47**	6.86								

*0.05显著性水平, **0.01显著性水平; r: 相关系数; R^2 : r的平方; ST: 符号检验; RE: 误差缩减值; CE: 有效系数; t: 乘积平均值。

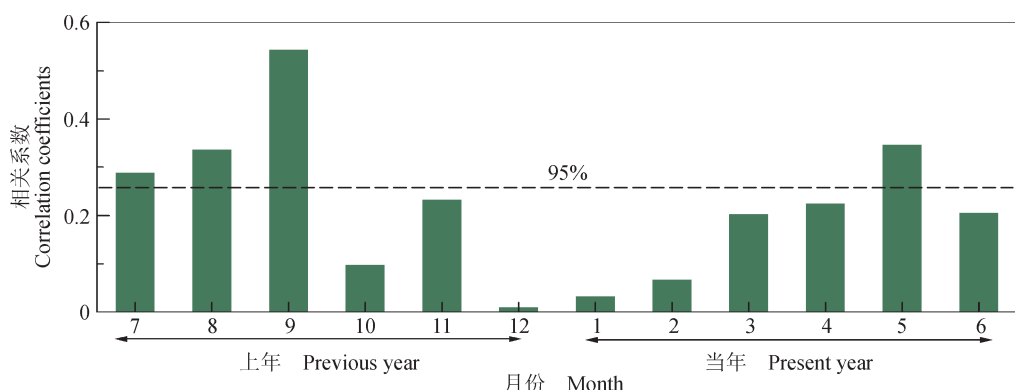
* significant level 0.05, ** significant level 0.01; r: correlation coefficient; R^2 : r square; ST: sign test; RE: reduction of error test; CE: coefficient of efficiency; t: product means test.



a: 器测 P_{JJ} 与格点 P_{JAS} 的空间相关; b: 树轮序列 (即重建 P_{JJ}) 与格点 P_{JAS} 的空间相关。 P_{JJ} 为上年七月至当年 6 月的年降水量, P_{JAS} 为上年七月至九月的降水量。两种空间相关模式对应较好, 进一步反映出亚洲夏季风北部边缘降水重建 P_{JJ} 的可靠性。图中仅显示 90% 置信水平以上的区域。

a: The instrumental P_{JJ} versus gridded P_{JAS} ; b: The tree-ring series (i.e., the reconstructed P_{JJ}) versus gridded P_{JAS} . P_{JJ} is the precipitation from previous July to current June, and P_{JAS} is the July—September precipitation of previous year. The two spatial patterns correspond well, reinforcing the notion that the reconstructed P_{JJ} is a reliable proxy for the precipitation of the northern margin of the Asian Summer Monsoon. Only areas above the 90% confidence level are shown.

图 4 CRU 降水格点数据 (CRU TS V4.01) 与 P_{JJ} 序列的空间相关分析 (1951—2012 年)
Fig.4 Correlation pattern between the CRU TS V4.01 grid precipitation data and P_{JJ} during the period 1951—2012



虚线代表 95% 置信限。

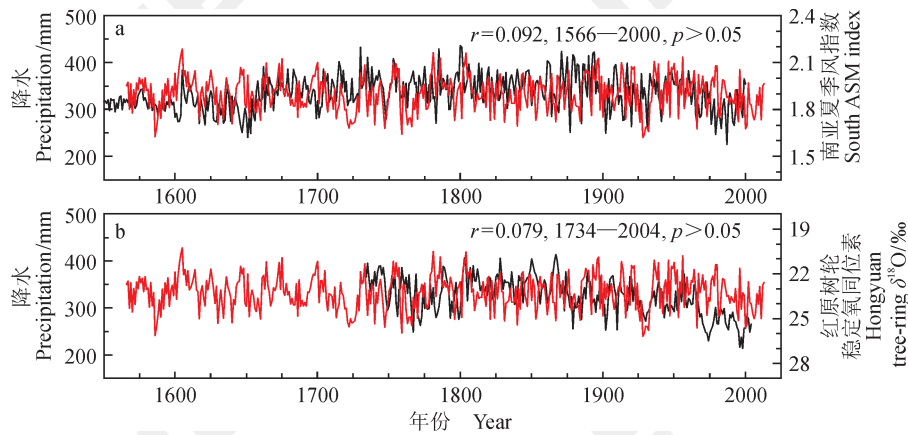
The dashed line denotes the 95% confidence limit. The reconstructed P_{JJ} time series is a proxy for the ASM.

图 5 树轮宽度序列与 39 个气象站月均降水观测值的相关性分析 (1952—2013 年)
Fig.5 Correlation between ring-width chronology and observed monthly averaged mean precipitation data from 39 stations in the fringe region (1951—2013)

2.2 历史文献及现有资料对重建 AMS 序列的校验

中国旱涝指数是基于具有气候描述的地方编年史等历史文献记录建立的。作为 ASM 代用指标的 P_{JJ} 序列, 捕捉到历史文献记录 (袁林, 1994; 中国气象灾害大典编委会, 2006) 和中国旱涝指数 (DWI) 序列 (中国气象科学研究院, 1981; 张德二等, 2003) 中的许多极端事件。发现当 DWI 增高时, P_{JJ} 呈下降趋势 (图 7a)。在 ASM 北部活动边缘带相关区域, 包括陕西、甘肃和宁夏地区在内的 1586/1587、1759、1928/1929 等几次大规模的严重干旱事件 (袁林, 1994; 中国气象灾

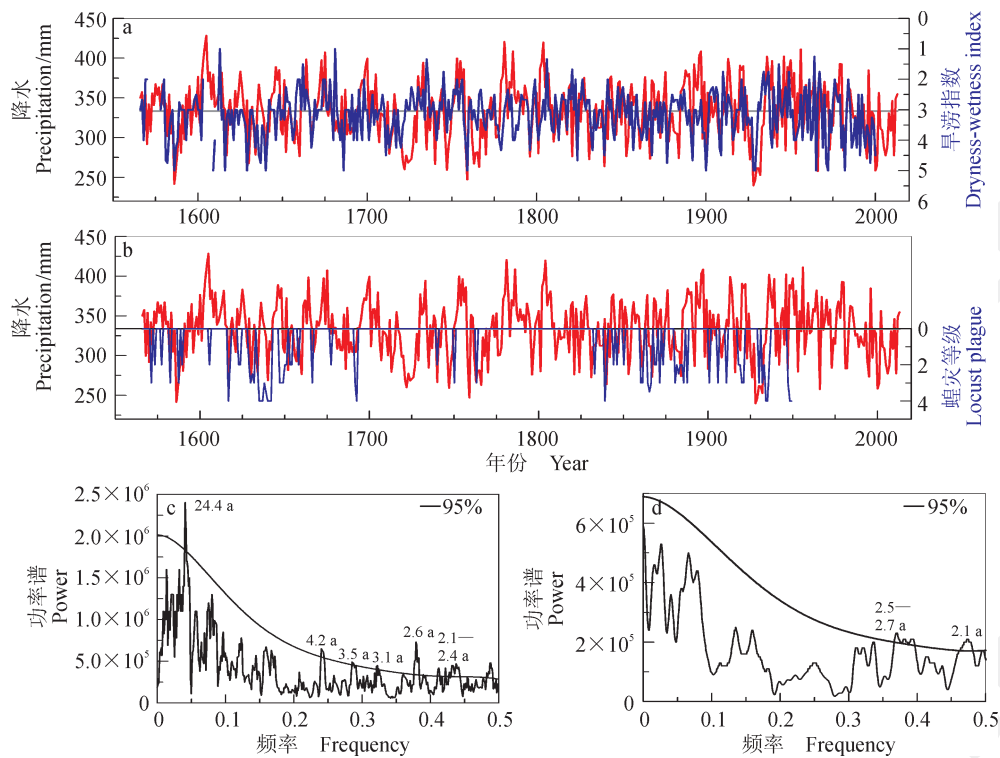
害大典编委会, 2006), 均被推设为 ASM 急剧减弱的结果。文献记载, 1586 年至 1587 年甘肃东部超过一半的人口逃离家园, 报道有人食人的现象发生; 1759 年, 粮食价格飞涨, 严重的饥荒困扰着甘肃地区 (袁林, 1994); 1928 年和 1929 年, 陕西、甘肃和宁夏三省 (区) 遭受严重干旱, 饥荒造成超过 50 万人死亡, 且有关于狗食人尸、整户自杀的记载 (袁林, 1994; 中国气象灾害大典编委会, 2006; Ge et al, 2016)。重建的 P_{JJ} 序列捕捉到了这些干旱事件 (表 5), 这为 ASM 减弱造成干旱提供了支持。



a: 南亚夏季风指数 (Shi et al., 2014; Shi et al., 2017); b: 青藏高原东缘红原树轮 $\delta^{18}\text{O}$ 序列 (Xu et al., 2012)。

a: South ASM index (Shi et al., 2014; Shi et al., 2017); b: tree ring $\delta^{18}\text{O}$ at Hongyuan, eastern edge of the Tibet Plateau (Xu et al., 2012).

图 6 本文降水重建序列 (红线) 与其他亚洲夏季风 (ASM) 序列 (黑线) 的对比
Fig.6 Comparisons between our reconstructed precipitation series (red line) and other series (black line) representing Asian Summer Monsoon (ASM)



a: P_{JJ} 与夏季风 (ASM) 边缘区旱涝指数 (来源于中国历史文献记录) 均值的对比 ($r=-0.26$, 1609—2000年, $p < 0.001$; 中国气象科学研究院, 1981; 张德二等, 2003)。灰色水平线为 ASM 边缘区 1566—2013 年 P_{JJ} 均值。b: ASM 边缘区 P_{JJ} 与历史蝗灾事件 (李钢, 2008)。

c: 基于 MTM (Multitaper Method) 谱分析得出的 1566—2013 年重建 P_{JJ} 序列的特征谱。d: 1914—2013 年重建 P_{JJ} 序列的特征谱。

图 7 重建 P_{JJ} 序列的特性。
Fig.7 Properties of the reconstructed P_{JJ} index

表 5 1566—2013 年的极干 ($\text{mean} - 2\sigma$) 年和极湿 ($\text{mean} + 2\sigma$) 年
Tab.5 Extreme drought ($\text{mean} - 2\sigma$) and wet ($\text{mean} + 2\sigma$) years during 1566—2013

极干年 Extremely drought year	降水量 Precipitation /mm	极湿年 Extremely wet year	降水量 Precipitation /mm
1928	240	1605	428
1586	241	1781	421
1929	246	1804	420
1759	247	1604	414
1932	253	1956	411
1966	258	1786	409
2000	258	1897	409
1747	259	1675	407

1566—2013 年的重建降水均值 (mean) 为 333 mm, 一个标准差 (1σ) 为 37 mm。定义降水量低于 296 mm (mean - 1σ) 为干旱年, 降水量大于 370 mm (mean + 1σ) 为湿润年。在过去 448 年中, 湿润年和干旱年分别占 15.6% (70 年) 和 16.1% (72 年)。定义降水量低于 259 mm (mean - 2σ) 为极干年, 大于 407 mm (mean + 2σ) 为极湿年。

The mean precipitation of the reconstruction is 333 mm for the period from 1566 to 2013 AD, and 1σ is 37 mm. We defined a dry year as having a value lower than 296 mm (mean - 1σ), and a wet year as having a value higher than 370 mm (mean + 1σ). In the past 448 years, wet and dry years accounted for 15.6 % (70 years) and 16.1 % (72 years), respectively. Extremely dry or wet years were defined as having a value lower than 259 mm (mean - 2σ) or higher than 407 mm (mean + 2σ).

泛滥的蝗虫吞噬了宝贵的粮食作物, 加剧了干旱对农作物产量的影响, 导致严重饥荒。历史记录的蝗灾均发生在 P_{JJ} 序列中的干旱年份 (图 7b), 特别

与极端干旱时段一致 (表 6)。因此, ASM 边缘带的蝗灾历史记录 (李钢, 2008; Tian et al., 2011) 进一步验证了 P_{JJ} 序列可作为 ASM 的代用序列。

表 6 极干年份里重建 P_{JJ} 、旱涝指数 (中国气象科学研究院, 1981; 张德二等, 2003) 以及
蝗灾指数 (李钢, 2008) 的对比

Tab.6 Comparisons between reconstructed P_{JJ} , the dryness/wetness index (Chinese Academy of Meteorological Sciences, 1981; Zhang et al, 2003), and the locust disaster index during some extreme years (Li, 2008)

极干年份 Extremely drought year	降水量 Precipitation /mm	旱 / 涝等级 * Dryness/Wetness grade*	蝗灾年份 Locust disaster year	蝗灾级别 ** Locust disaster level**
1928	240	5	1928	3
1586	241	5	1587	3
1929	246	5	1930	4
1759	247	5	1761	3
1932	253	3	1932	2
1966	258	3		
2000	258	5		
1747	259	4	1748	3

* 20 世纪 20 年代, 数百名中国气候学家查阅了全国范围内 2200 余种地方志, 编录史料超过二百二十万字 (数据), 将过去 510 年的干湿状况划分为 5 个等级 (中国气象科学研究院, 1981): 1 级——涝; 2 级——偏涝; 3 级——正常; 4 级——偏旱; 5 级——旱。

** 蝗灾级别定义 (李钢, 2008): 1 级——出现级, 仅有局部一两个小区域发现一代蝗虫, 几乎没有造成危害 (能收八九成以上)。2 级——干扰级, 两个或两个以上区域发生一代蝗灾, 对农业生产有危害 (可收六到八成)。3 级——危害级, 多个区域多次发生一到两代较大蝗灾, 有迁飞扩散能力, 对农业生产造成较大破坏 (仅收三到五成), 灾区生产难以恢复。4 级——灾难级, 多个区域或几近全国的范围发生两代以上特大蝗灾, 频繁迁飞扩散, 对农业生产 (绝收, 或仅余一二成) 和百姓生活带来巨大灾难, 往往与饥荒、瘟疫、战争相伴。

* During the 1920s, hundreds of Chinese climatologists processed more than 2200 local annals and many other historical writings nationwide and abstracted more than 2200000 characters (data). The degree of annual dryness and wetness during the last 510 years was classified into 5 grades (Chinese Academy of Meteorological Sciences, 1981): Grade 1—very wet; Grade 2—wet; Grade 3—normal; Grade 4—dry; and Grade 5—drought.

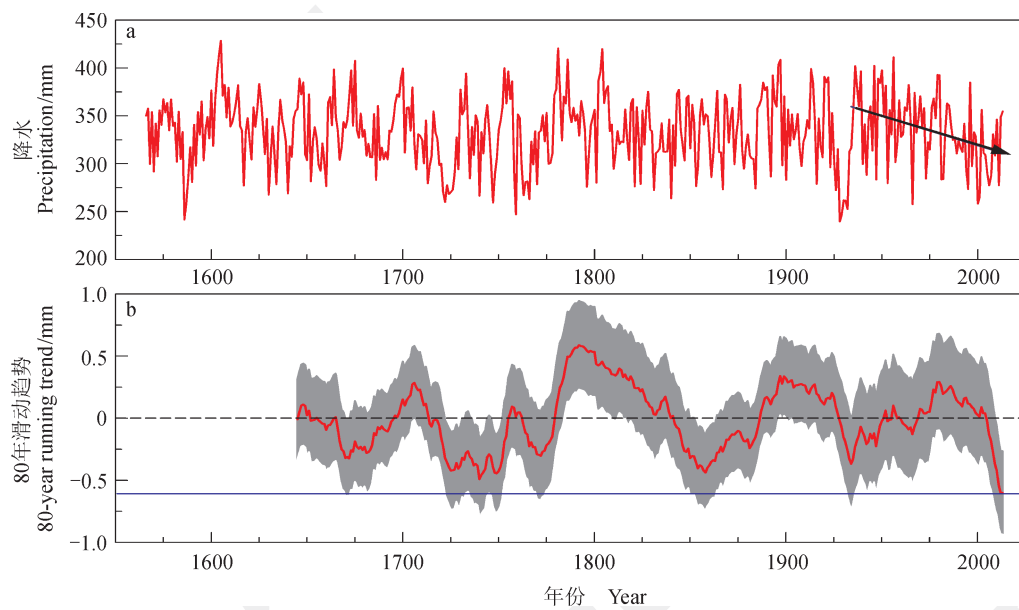
** The definition level of locust plagues (Li, 2008): Grade 1—Occurrence grade. The first generation of locusts appeared in only one or two small areas, and there was almost no harm to agriculture output. Crop harvest reached about 80%—90%. Grade 2—Impact grade. The first generation of locusts appeared in two or more areas, and there was harm to agriculture, with crop harvest about 60%—80%. Grade 3—Hazard grade. The first and the second generation of locusts appeared in many areas, and there was huge damage to agricultural production. Crops harvest was about 30%—50%, and production was difficult to restore. Grade 4—Disastrous grade. More than two generations of locusts appeared in multiple areas to almost national scope. There were enormous disasters to agriculture output with no or less than 10%—20% harvest, and the people could not survive. The disaster was often accompanied by famine, plague and war.

P_{JJ} 重建序列中的显著变化特征(图7), 在其他基于不同代用指标的古气候重建序列中也有明确体现(Zhang et al, 2008; Qian et al, 2011)。如重建序列反映的24年周期(图7c), 与另一条基于中国东部6种夏季干湿分布型重建的过去千年东亚夏季风干湿分布型指数序列(Qian et al, 2011)所包含的23年周期相吻合; P_{JJ} 序列的2.5—2.8年周期则反映了亚洲季风变化的典型周期特征(Wu and Kirtman, 2004)。尽管Qian et al(2011)的指数序列覆盖时段更长, 但它只是基于六种模式的对ASM的定性描述, 而本文的重建序列则是对ASM的定量反映。

2.3 近年来ASM减弱与人为气溶胶的影响

本文重建序列涉及到近年来关于气候变化的争议, 特别是ASM对气候变暖如何响应的问题。因此这个重建序列的作用远不止用于直接检验、证实和再现历史事件。现代降水观测记录显示

ASM存在减弱趋势(如: 30—40年减弱趋势; Xu et al, 2006; Wang et al, 2012), P_{JJ} 序列在近几十年来同样显示出了下降趋势, 但观测记录涵盖的时段则相对较短。为了找出ASM最明显且持续时间最长的减弱趋势, 分别计算了1566—2013年 P_{JJ} 重建序列50年、55年、60年、65年、70年、75年、80年、85年和90年等各个步长的滑动趋势计算。结果发现近几十年中, 持续时间最长、最显著的下降趋势出现在80年滑动趋势分析中。因此, 在80年滑动窗口下, 1934—2013年显著的80年下降趋势(图8a)是整个448年间最大的(图8b), 且80年的下降趋势与印度季风区近100年来降水显著减弱的趋势相似(Xu et al, 2016)。这是因为本研究的降水同时代表了印度季风和东亚季风的变化, 尽管 P_{JJ} 序列在近100年呈下降趋势(约 $0.14 \text{ mm} \cdot \text{a}^{-1}$), 但是并未超过95%的显著性水平。



a: 过去四个世纪以来的 P_{JJ} 重建(红色曲线)。倾斜黑线指示 1934—2013 年 P_{JJ} 的 80 年下降趋势。b: 重建 P_{JJ} 的 80 年滑动序列(红线)。灰色区域代表 95% 置信区间。蓝色水平线代表最大的 80 年降水减少量, 约 $0.62 \text{ mm} \cdot \text{a}^{-1}$ 。
a: the reconstructed P_{JJ} during the past four centuries (red curve). The sloping black line denotes an 80-year decreasing trend of P_{JJ} during the period 1934 to 2013. b: eighty-year running trend (red line) for reconstructed P_{JJ} . The gray area denotes the 95% confidence intervals. The blue horizontal line indicates the greatest 80-year decline in precipitation of approximately $0.62 \text{ mm} \cdot \text{a}^{-1}$.

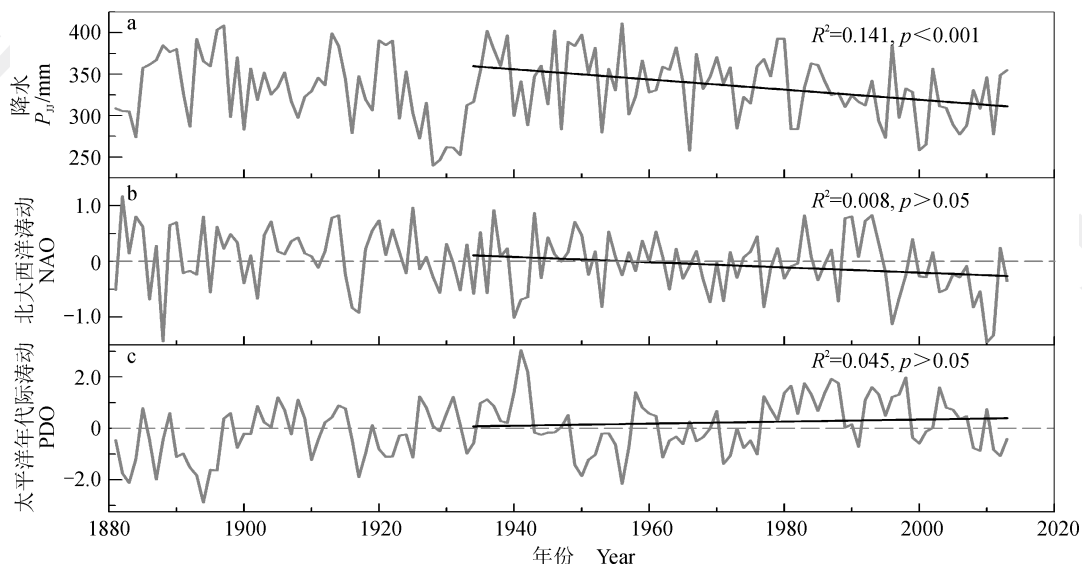
图 8 P_{JJ} 全序列重建
Fig.8 The reconstructed P_{JJ} time series

在不同的外部强迫下, 由温室效应主导的辐射强迫模型的预测结果为: 陆地的升温速率高于海洋, 海陆热力差异会增加(Christensen et al, 2013), ASM在近几十年会有所增强, 但这与本文结果不一

致, 因此极可能有其他强迫导致ASM强度减弱。在寻找其动力学原因时, 发现无论是PDO(Watanabe and Yamazaki, 2014)还是NAO(Lu et al, 2006)都无法对80年减弱趋势(图9)做出解释。

因此,考虑到另一个因素,即不断增加的人为气溶胶占主导地位的强迫(Bollasina et al, 2011)。尽管西亚上空的黑碳排放增加了印度次大陆的季风前期降水,但却抑制了整个东亚地区的季风前期降水(Lau et al, 2006),同时硫酸盐排放也已被证

实会迫使ASM强度下降(Menon et al, 2002; Lau et al, 2006)。因而,假设重建 P_{JJ} 序列中ASM表现的80年减弱趋势是由硫酸盐气溶胶所主导,即人为气溶胶的增加在ASM减弱过程中抵消了温室气体增加导致的ASM增强效应。



a: 亚洲夏季风北部边缘带重建 P_{JJ} 。b: 上年7月到当年6月的NAO指数(Lu et al, 2006)。c: 上年7月到当年6月的PDO指数(Watanabe and Yamazaki, 2014)。黑线代表1934—2013年的线性趋势。该对比表明, P_{JJ} 的下降趋势并非由NAO或PDO引起。

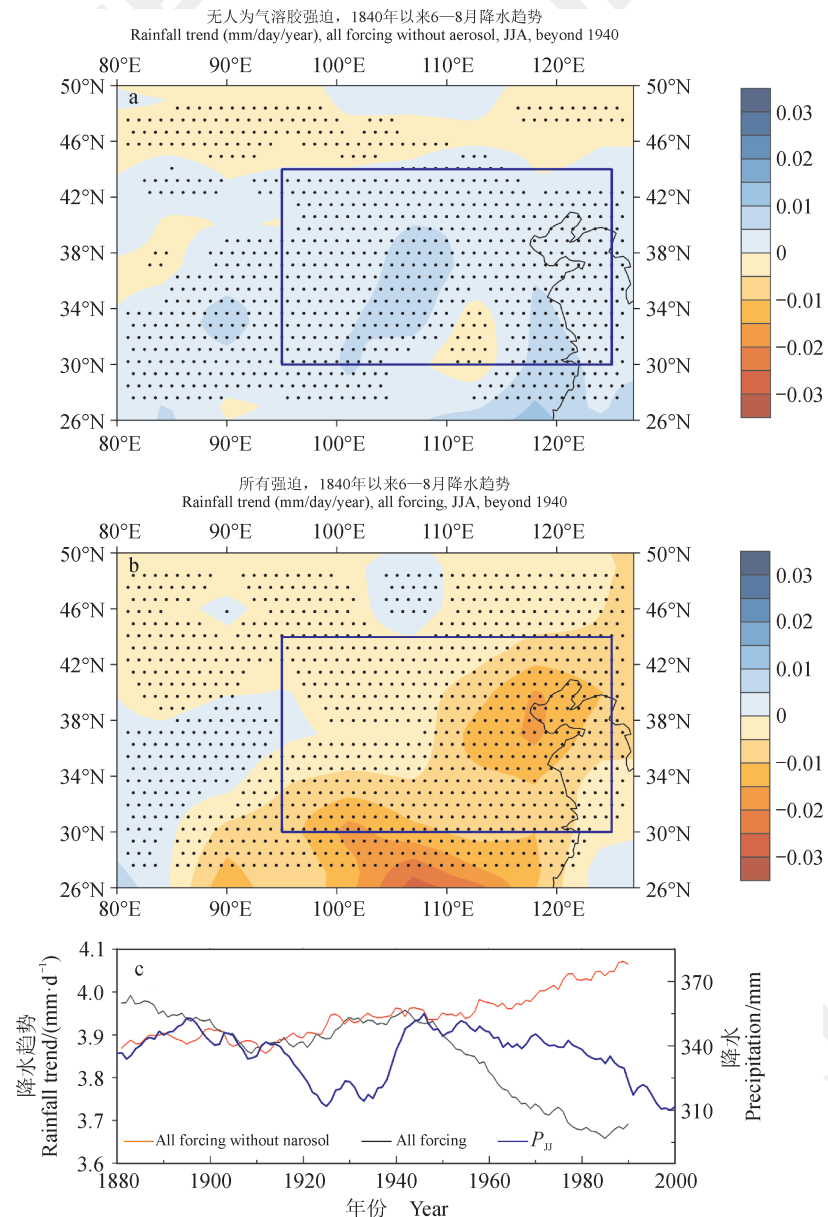
a: the reconstructed P_{JJ} in the fringe region of the Asian Summer Monsoon. b: monthly North Atlantic Oscillation (NAO) index (Lu et al, 2006) from previous July to current June. c: monthly Pacific Decadal Oscillation (PDO) index (Watanabe and Yamazaki, 2014) from previous July to current June. The black lines represent their linear trends during the period 1934—2013. This demonstrates that the decreasing trend of P_{JJ} is not caused by any trends of NAO and PDO.

图9 1881—2013年重建 P_{JJ} 、太平洋十年涛动指数(PDO)及北大西洋涛动指数(NAO)

Fig.9 The reconstructed P_{JJ} , Pacific Decadal Oscillation and North Atlantic Oscillation during the period 1881—2013

运用CSIRO模式(Rotstain et al, 2007)中的两种耦合气候模型来验证上述假设,每组模型都包含8个耦合因子,时间范围为1871—1999年。第一组模型包括随时间变化的所有强迫因素,如:全球太阳辐射强迫、温室气体、臭氧、火山活动和人为气溶胶排放等因素。第二组除了将人为气溶胶排放量设定为工业化前水平的常量外,其他与第一组相同。对气溶胶的所有直接和间接影响都考虑在内并进行参数化。正如Rotstain et al (2007)指出的那样:“该模型设计了一个全面的和相互作用的气溶胶方案,包含硫酸盐和碳质气溶胶、矿物粉尘、海盐和平流层火山气溶胶的排放。”二战后,从1940年开始全球排放量经历了大幅增长,到1980年前后除亚洲外世界各地的硫酸盐排放量都有所减少,而到目前为止亚洲的排放量却在

持续增加(Smith et al, 2011)。将两组模型的总体均值进行比较,结果表明,在包括ASM边缘带的中国大部分地区,1940年以来的夏季降水在没有人为硫酸盐气溶胶辐射强迫的情况下都会增加(图10a),而当加入硫酸盐气溶胶强迫时,ASM区域(包括ASM边缘带)降水则会显著减少(图10b)。在中国北方及AMS活动边缘区域,人为硫酸盐气溶胶的影响在21年滑动平均序列上表现十分明显。1920—1940年的降水低值与辐射强迫变化无关(图10c),很可能是由正相位PDO导致的(图9)。在这个模型中,下降趋势的起始时间大约从1940年开始(图10c),这与 P_{JJ} 重建序列中所表现出的时间大致对应。因此,北半球人为硫酸盐气溶胶排放量的增加可能是导致本文重建ASM序列中显著80年减弱趋势的主要因素。



a: 包含除人为气溶胶以外的所有强迫因素。b: 包含全球太阳辐射、温室气体、臭氧、火山活动和人为气溶胶排放在内的所有强迫因素。蓝色矩形框为中国北方区域，黑点代表降水趋势超过95%显著性水平。c: 中国北方区域 P_{JJA} 与降水趋势对比。黑线和红线均代表根据气候模式模拟的中国北方区域降水变化的21年滑动平均序列，蓝线为 P_{JJA} 21年滑动平均序列。结果显示1940—2013年的 P_{JJA} 下降趋势可能是由人为气溶胶引起。JJA指六月至八月。

a: All forcing but without anthropogenic aerosols. b: All forcing including global emissions of solar irradiance, greenhouse gases, ozone, volcanic aerosols, and anthropogenic aerosols. Blue rectangular outline is the northern regions of China, and the black dot indicates that the rainfall trend passes the 95% significant level. c: Comparisons between P_{JJA} and rainfall trends for the northern regions of China. The black and red lines indicate the 21-year running averages of rainfall changes of the northern regions of China simulated from climate model, and the blue line is the P_{JJA} series after applying 21-year running averages. The result shows that the decreasing trend in P_{JJA} from 1940 to 2013 is potentially contributed by anthropogenic aerosols. JJA=June—August.

图10 用耦合气候模式模拟1940年以来北方夏季降水趋势(Rotstain et al., 2007)
Fig.10 Boreal summer rainfall trends since 1940 simulated by a coupled climate model (Rotstain et al., 2007)

3 讨论与结论

本文基于ASM活动边缘带10个对降水变化响应显著的树轮年表,重建了一条可以反映过去

448年ASM强度变化的降水序列。与以往研究相比,其重要性不仅体现在具有更高的重建方差解释量,还体现在具有更宽广的空间场,能直接代

表 ASM 强度的变化。本文的重建序列是研究 448 年以来 ASM 变化的重要资料。重建 ASM 序列再现了许多重要的 ASM 特征 (Qian et al, 2011; 如: 24 年周期)、已知的历史极端气候事件 (Ge et al, 2016)，并对了解未知气候事件提供了可能途径 (Tian et al, 2011)。

此外，重建结果可以对近年来关于 ASM 变化的争论提供论据 (Zhu et al, 2012b)，并对评价人为辐射强迫因素的重要性提供支持 (Song et al, 2014)。本研究发现了在过去 448 年中前所未有的、最为强烈的、显著的持续 80 多年的 ASM 强度减弱趋势，这与受温室效应影响 ASM 应该增强的预期大相径庭。两组气候模型实验（有 / 无人为气溶胶排放增加，每组运行 10 次）对比表明，这一前所未有的减弱趋势很可能是由人为硫酸盐气溶胶排放增加引起，人为气溶胶硫酸盐排放引起的 ASM 减弱效应可能抵消了温室气体引发的 ASM 增强效应。模拟是识别造成 ASM 减弱可能原因的唯一方法，实验结果为上述假设提供了其他方法无法提供的支持。Song et al (2014) 首次定量比较了 1958—2001 年所有导致 ASM 减弱的外部作用中人为气溶胶的影响。这项工作进一步证实了人为气溶胶在 1934—2013 年，这一较长时间内对 ASM 减弱的作用。因此，认为北半球人为硫酸盐气溶胶排放量的增加可能是导致近 80 年来 ASM 减弱的主要因素，而此前，在没有人为气溶胶排放的历史时期，PDO 和 NAO 等其他因素可能对 ASM 减弱 / 增强产生影响。

综上所述，重建的 ASM 时间序列将在了解季风活动边缘带过去气候变化、研究当前气候变化检测和归因、评估人为强迫和预测未来气候变化等方面起到重要作用。

参考文献

- 李 钢 . 2008. 历史时期中国蝗灾记录特征及其环境意义集成研究 [D]. 兰州 : 兰州大学 . [Li G. 2008. An integrated study on record characteristics and environmental significance of locust plagues in China during the historical period [D]. Lanzhou: Lanzhou University.]
- 宋慧明, 刘 禹, 梅若晨, 等 . 2017. 甘肃竺尼山油松树轮宽度气候响应 [J]. 地球环境学报, 8(2): 119–126. [Song H M, Liu Y, Mei R C, et al. 2017. The climatic response of *Pinus tabulaeformis* Carr. in Mt. Zhuni, Gansu [J]. *Journal of Earth Environment*, 8(2): 119–126.]
- 袁 林 . 1994. 西北灾荒史 [M]. 兰州 : 甘肃人民出版社 . [Yuan L. 1994. The records of disasters in Northwest China [M]. Lanzhou: Gansu People's Publishing House.]
- 张德二, 李小泉, 梁有叶 . 2003. 《中国近五百年旱涝分布图集》的再续补 (1993—2000 年) [J]. 应用气象学报, 14(3): 379–388. [Zhang D E, Li X Q, Liang Y Y. 2003. Supplement for “Yearly charts of dryness/wetness in China for the last 500-year period” [J]. *Journal of Applied Meteorological Science*, 14(3): 379–388.]
- 中国气象科学研究院 . 1981. 中国近 500 年旱涝分布图集 [M]. 北京 : 地图出版社 . [Chinese Academy of Meteorological Sciences. 1981. Yearly charts of dryness/wetness in China for the last 500-year period [M]. Beijing: SinoMaps Press.]
- 中国气象灾害大典编委会 . 2006. 中国气象灾害大典 [M]. 北京 : 气象出版社 . [Compilation of China meteorological disaster Canon. 2006. China meteorological disaster Canon [M]. Beijing: China Meteorological Press.]
- Bollasina M A, Ming Y, Ramaswamy V. 2011. Anthropogenic aerosols and the weakening of the South Asian summer monsoon [J]. *Science*, 334(6055): 502–505.
- Cai W J, Li K, Liao H, et al. 2017. Weather conditions conducive to Beijing severe haze more frequent under climate change [J]. *Nature Climate Change*, 7(4): 257–262.
- Christensen J H, Krishna Kumar K, Aldrian E, et al. 2013. Climate phenomena and their relevance for future regional climate change [C]// Stocker T F, Qin D, Plattner G K, et al. *Climate change 2013: the physical science basis. Contribution of Working Group I to the Fifth Assessment Report of the Intergovernmental Panel on Climate Change*. Cambridge, UK and New York: Cambridge University Press: 1217–1308.
- Cook E R and Kairiukstis L A. 1990. *Methods of dendrochronology: Applications in the environmental sciences* [M]. Dordrecht: Kluwer Academic Publishers.
- Cook E R, Meko D M, Stahle D W, et al. 1999. Drought reconstructions for the continental United States [J]. *Journal of Climate*, 12(4): 1145–1162.
- Ding Y H, Chan J C L. 2005. The East Asian summer monsoon: an overview [J]. *Meteorology and Atmospheric Physics*, 89(1/2/3/4): 117–142.
- Ding Y H, Wang Z Y, Sun Y. 2008. Inter-decadal variation of the summer precipitation in East China and its association with decreasing Asian summer monsoon. Part I : Observed evidences [J]. *International Journal of Climatology*, 28(9):

- 1139–1161.
- Fang K Y, Gou X H, Chen F H, et al. 2010. Tree-ring based drought reconstruction for the Guiqing Mountain (China): linkages to the Indian and Pacific Oceans [J]. *International Journal of Climatology*, 30(8): 1137–1145.
- Feng J, Wang L, Chen W. 2014. How does the East Asian summer monsoon behave in the decaying phase of El Niño during different PDO phases? [J]. *Journal of Climate*, 27(7): 2682–2698.
- Fritts H C. 1976. Tree rings and climate [M]. London: Academic Press.
- Fritts H C. 1991. Reconstructing large-scale climatic patterns from tree-ring data [M]. Tucson: The University of Arizona Press.
- Ganguly D, Rasch P J, Wang H L, et al. 2012. Climate response of the South Asian monsoon system to anthropogenic aerosols [J]. *Journal of Geophysical Research: Atmospheres*, 117(D13209). DOI: 10.1029/2012JD017508.
- Ge Q S, Zheng J Y, Hao Z X, et al. 2016. Recent advances on reconstruction of climate and extreme events in China for the past 2000 years [J]. *Journal of Geographical Sciences*, 26(7): 827–854.
- Grießinger J, Bräuning A, Helle G, et al. 2011. Late Holocene Asian summer monsoon variability reflected by $\delta^{18}\text{O}$ in tree-rings from Tibetan junipers [J]. *Geophysical Research Letters*, 38(L03701). DOI: 10.1029/2010GL045988.
- Kim M J, Yeh S W, Park R J. 2016. Effects of sulfate aerosol forcing on East Asian summer monsoon for 1985—2010 [J]. *Geophysical Research Letters*, 43(3): 1364–1372.
- Lau K M, Kim K M. 2006. Observational relationships between aerosol and Asian monsoon rainfall, and circulation [J]. *Geophysical Research Letters*, 33(L21810). DOI: 10.1029/2006GL027546.
- Lau K M, Kim M K, Kim K M. 2006. Asian summer monsoon anomalies induced by aerosol direct forcing: the role of the Tibetan Plateau [J]. *Climate Dynamics*, 26(7/8): 855–864.
- Li J B, Cook E R, D'Arrigo R, et al. 2008. Common tree growth anomalies over the northeastern Tibetan Plateau during the last six centuries: implications for regional moisture change [J]. *Global Change Biology*, 14(9): 2096–2107.
- Li J P, Zeng Q C. 2002. A unified monsoon index [J]. *Geophysical Research Letters*, 29(8). DOI: 10.1029/2001GL013874.
- Li X Q, Ting M F, Li C H, et al. 2015. Mechanisms of Asian summer monsoon changes in response to anthropogenic forcing in CMIP5 models [J]. *Journal of Climate*, 28(10): 4107–4125.
- Li Z Q, Lau W K M, Ramanathan V, et al. 2016. Aerosol and monsoon climate interactions over Asia [J]. *Reviews of Geophysics*, 54(4): 866–929.
- Liu J B, Rühland K M, Chen J H, et al. 2017. Aerosol-weakened summer monsoons decrease lake fertilization on the Chinese Loess Plateau [J]. *Nature Climate Change*, 7(3): 190–194.
- Liu Y, Cai Q F, Shi J F, et al. 2005. Seasonal precipitation in the south-central Helan Mountain region, China, reconstructed from tree-ring width for the past 224 years [J]. *Canadian Journal of Forest Research*, 35(10): 2403–2412.
- Liu Y, Lei Y, Sun B, et al. 2013a. Annual precipitation variability inferred from tree-ring width chronologies in the Changling-Shoulu region, China, during AD 1853–2007 [J]. *Dendrochronologia*, 31(4): 290–296.
- Liu Y, Lei Y, Sun B, et al. 2013b. Annual precipitation in Liancheng, China, since 1777 AD derived from tree rings of Chinese pine (*Pinus tabulaeformis* Carr.) [J]. *International Journal of Biometeorology*, 57(6): 927–934.
- Liu Y, Sun B, Song H M, et al. 2013c. Tree-ring-based precipitation reconstruction for Mt. Xinglong, China, since AD 1679 [J]. *Quaternary International*, 283: 46–54.
- Liu Z Y, Wen X Y, Brady E C, et al. 2014. Chinese cave records and the East Asia summer monsoon [J]. *Quaternary Science Reviews*, 83: 115–128.
- Lu R Y, Dong B W, Ding H. 2006. Impact of the Atlantic multidecadal oscillation on the Asian summer monsoon [J]. *Geophysical Research Letters*, 33(L24701). DOI: 10.1029/2006GL027655.
- Ma Y Y, Liu Y, Song H M, et al. 2015. A standardized precipitation evapotranspiration index reconstruction in the Taihe Mountains using tree-ring widths for the last 283 years [J]. *PLoS ONE*, 10(7): e0133605. DOI: 10.1371/journal.pone.0133605.
- Menon S, Hansen J, Nazarenko L, et al. 2002. Climate effects of black carbon aerosols in China and India [J]. *Science*, 297(5590): 2250–2253.
- Piao S L, Ciais P, Huang Y, et al. 2010. The impacts of climate change on water resources and agriculture in China [J]. *Nature*, 467(7311): 43–51.
- Qian W H, Zhu Y F, Tang S Q. 2011. Reconstructed index of summer monsoon dry-wet modes in East Asia for the last millennium [J]. *Chinese Science Bulletin*, 56(28/29): 3019–3027.

- Rotstayn L D, Cai W J, Dix M R, et al. 2007. Have Australian rainfall and cloudiness increased due to the remote effects of Asian anthropogenic aerosols? [J]. *Journal of Geophysical Research*, 112(D09202). DOI: 10.1029/2006JD007712.
- Shi F, Fang K Y, Xu C X, et al. 2017. Interannual to centennial variability of the South Asian summer monsoon over the past millennium [J]. *Climate Dynamics*, 49(7/8): 2803–2814.
- Shi F, Li J P, Wilson R J S. 2014. A tree-ring reconstruction of the South Asian summer monsoon index over the past millennium [J]. *Scientific Reports*, 4: 6739.
- Smith S J, van Aardenne J, Klimont Z, et al. 2011. Anthropogenic sulfur dioxide emissions: 1850—2005 [J]. *Atmospheric Chemistry and Physics*, 11(3): 1101–1116.
- Song F F, Zhou T J, Qian Y. 2014. Responses of East Asian summer monsoon to natural and anthropogenic forcings in the 17 latest CMIP5 models [J]. *Geophysical Research Letters*, 41(2): 596–603.
- Song H M, Liu Y. 2011. PDSI variations at Kongtong Mountain, China, inferred from a 283-year *Pinus tabulaeformis* ring width chronology [J]. *Journal of Geophysical Research*, 116(D22111). DOI:10.1029/2011JD016220.
- Sun C F, Liu Y, Song H M, et al. 2018. Tree-ring-based precipitation reconstruction in the source region of Weihe River, northwest China since AD 1810 [J]. *International Journal of Climatology*, 38(8): 3421–3431.
- Tian H D, Stige L C, Cazelles B, et al. 2011. Reconstruction of a 1,910-y-long locust series reveals consistent associations with climate fluctuations in China [J]. *Proceedings of the National Academy of Sciences of the United States of America*, 108(35): 14521–14526.
- Ueda H, Kamae Y, Hayasaki M, et al. 2015. Combined effects of recent Pacific cooling and Indian Ocean warming on the Asian monsoon [J]. *Nature Communications*, 6: 8854.
- Waliser D E, Jin K, Kang I S, et al. 2003. AGCM simulations of intraseasonal variability associated with the Asian summer monsoon [J]. *Climate Dynamics*, 21(5/6): 423–446.
- Wang B, Fan Z. 1999. Choice of south Asian summer monsoon indices [J]. *Bulletin of the American Meteorological Society*, 80(4): 629–638.
- Wang B, Wu R G, Lau K M. 2001. Interannual variability of the Asian summer monsoon: contrasts between the Indian and the western North Pacific-east Asian monsoons [J]. *Journal of Climate*, 14(20): 4073–4090.
- Wang B, Wu Z W, Li J P, et al. 2008. How to measure the strength of the east Asian summer monsoon [J]. *Journal of Climate*, 21(17): 4449–4463.
- Wang B. 2006. The Asian monsoon [M]. Chichester, UK: Praxis Publishing Ltd.: 1–787.
- Wang H J. 2001. The weakening of the Asian monsoon circulation after the end of 1970's [J]. *Advances in Atmospheric Sciences*, 18(3): 376–386.
- Watanabe T, Yamazaki K. 2014. Decadal-scale variation of South Asian summer monsoon onset and its relationship with the Pacific Decadal Oscillation [J]. *Journal of Climate*, 27(13): 5163–5173.
- Wigley T M L, Briffa K R, Jones P D. 1984. On the average value of correlated time series, with applications in dendroclimatology and hydrometeorology [J]. *Journal of Climatology & Applied Meteorology*, 23(2): 201–213.
- Wu G X, Li Z Q, Fu C B, et al. 2016. Advances in studying interactions between aerosols and monsoon in China [J]. *Science China Earth Sciences*, 59(1): 1–16.
- Wu R G, Kirtman B P. 2004. The tropospheric biennial oscillation of the monsoon-ENSO system in an interactive ensemble coupled GCM [J]. *Journal of Climate*, 17(8): 1623–1640.
- Xu H, Hong Y T, Hong B. 2012. Decreasing Asian summer monsoon intensity after 1860 AD in the global warming epoch [J]. *Climate Dynamics*, 39(7/8): 2079–2088.
- Xu H, Lan J H, Sheng E G, et al. 2016. Hydroclimatic contrasts over Asian monsoon areas and linkages to tropical Pacific SSTs [J]. *Scientific Reports*, 6: 33177.
- Xu M, Chang C P, Fu C B, et al. 2006. Steady decline of east Asian monsoon winds, 1969—2000: Evidence from direct ground measurements of wind speed [J]. *Journal of Geophysical Research*, 111(D24111). DOI: 10.1029/2006JD007337.
- Zhang P Z, Cheng H, Edwards R L, et al. 2008. A test of climate, sun, and culture relationships from an 1810-year Chinese cave record [J]. *Science*, 322(5903): 940–942.
- Zhu C W, Wang B, Qian W H, et al. 2012b. Recent weakening of northern East Asian summer monsoon: A possible response to global warming [J]. *Geophysical Research Letters*, 39(L09701). DOI: 10.1029/2012GL051155.
- Zhu J L, Liao H, Li J P. 2012a. Increases in aerosol concentrations over eastern China due to the decadal-scale weakening of the East Asian summer monsoon [J]. *Geophysical Research Letters*, 39(L09809). DOI: 10.1029/2012GL051428.